Published in final edited form as:
Cell Metab. 2010 May 5; 11(5): 402–411. doi:10.1016/j.cmet.2010.03.012.

Resistance to High-fat Diet-induced Obesity and Insulin Resistance in Mice with Very Long-chain Acyl-CoA Dehydrogenase Deficiency

Dongyan Zhang[1], **Jennifer Christianson**[1], **Zhen-Xiang Liu**[1], **Liqun Tian**[4], **Cheol Soo Choi**[2], **Susanne Neschen**[1], **Jianying Dong**[1], **Philip A. Wood**[4,5], and **Gerald I. Shulman**[1,2,3]

[1]Howard Hughes Medical Institute, Yale University School of Medicine, New Haven, CT

[2]Department of Internal Medicine, Yale University School of Medicine, New Haven, CT

[3]Department of Cellular & Molecular Physiology, Yale University School of Medicine, New Haven, CT

[4]Department of Genetics, University of Alabama at Birmingham, Birmingham, AL

[5]Diabetes and Obesity Research Center, Sanford-Burnham Medical Research Institute, Orlando, FL

Abstract

Mitochondrial fatty acid oxidation provides an important energy source for cellular metabolism and decreased mitochondrial fatty acid oxidation has been implicated in the pathogenesis of type 2 diabetes. Paradoxically, mice with an inherited deficiency of the mitochondrial fatty acid oxidation enzyme, very long chain acyl-CoA dehydrogenase (VLCAD), manifested increased fatty acid oxidation in liver, muscle and brown adipose tissue and a lower whole body respiratory quotient compared to WT mice. Moreover, VLCAD$^{-/-}$ mice were protected from fat-induced liver and muscle insulin resistance, which was associated with reduced intracellular diacylglycerol content and decreased activity of protein kinase Cε and protein kinase Cθ in liver and muscle respectively. The increased insulin sensitivity in the VLCAD$^{-/-}$ mice was associated with increased liver and muscle AMPK activity and increased PPARα expression in muscle and brown adipose tissue. Taken together these data suggest that VLCAD$^{-/-}$ mice were protected from diet-induced obesity and insulin resistance due to chronic activation of AMPK (liver and muscle) and PPARα (muscle and BAT) activity resulting in increased fatty acid oxidation and decreased intramyocellular and hepatocellular diacylglycerol content. Furthermore these data demonstrate that mitochondrial dysfunction can paradoxically result in increased insulin sensitivity due to these compensatory mechanisms.

Address correspondence to: Gerald I. Shulman M.D. Ph.D. Howard Hughes Medical Institute Yale University School of Medicine S269 TAC, Box 9812 Yale University School of Medicine New Haven, CT 06510 Phone: (203) 785-5447 Fax: (203) 737-4059 gerald.shulman@yale.edu Philip A. Wood, DVM. Ph.D. Diabetes and Obesity Research Center Sanford-Burnham Medical Research Institute 6400 Sanger Rd Orlando, FL 32827 Phone: (407) 745-2083 Fax: (407) 745-2001 pwood@burnham.org.

Introduction

Mitochondrial dysfunction with impaired skeletal muscle oxidative phosphorylation has been implicated in the pathogenesis of insulin resistance and type 2 diabetes mellitus (T2DM) (Kelley et al., 2002, Petersen et al., 2003; Mootha et al., 2003; Patti et al., 2003; Petersen et al., 2004). Mitochondrial dysfunction resulting from a deficiency of long chain acyl-CoA dehydrogenase (LCAD) caused fatty liver and hepatic insulin resistance in mice (Zhang et al., 2007). A closely related enzyme of the same pathway, very long chain acyl-CoA dehydrogenase (VLCAD) is a mitochondrial membrane associated enzyme that is upstream of long chain acyl-CoA dehydrogenase in the mitochondrial fatty acid β-oxidation spiral. Previous studies in humans have found that VLCAD deficiency resulted in reduced fatty acid oxidation and was associated with fasting intolerance, Reye syndrome-like disease, cardiac and skeletal muscle disease (Cox et al., 2001). To further investigate the relationship between fatty acid oxidation enzyme deficiency and insulin resistance, we performed metabolic studies on VLCAD deficient ($VLCAD^{-/-}$) mice after high-fat feeding. Surprisingly, we found that the $VLCAD^{-/-}$ mice were resistant to high-fat diet induced obesity and insulin resistance with a mechanism related to activation of AMPK in liver and skeletal muscle and a compensatory increase in fatty acid oxidation.

Results

$VLCAD^{-/-}$ mice are resistant to high-fat diet induced obesity due to decreased energy intake and decreased respiratory quotient

Preliminary hyperinsulinemic-euglycemic clamp study of the $VLCAD^{-/-}$ mice fed standard diet showed no difference in insulin sensitivity compared to WT mice (Supplemental Data, Fig.1). To investigate why a major fatty acid oxidation enzyme deficiency did not lead to insulin resistance, we subjected the $VLCAD^{-/-}$ mice to a high-fat diet. Interestingly, two weeks of *ad lib* feeding of the high fat diet caused a 40% increase in body weight in the WT mice, while only causing a 10% increase in body weight in the $VLCAD^{-/-}$ mice within the same period (Fig. 1A, Day 14). Another 3 months of high-fat feeding led to further body weight gains in both groups with the WT gaining slightly more than the $VLCAD^{-/-}$ mice (Fig. 1A, $P<0.05$ from day 9 to day 100). Food intake measurements showed that $VLCAD^{-/-}$ mice had significantly less food intake than WT mice for the first two weeks of the feeding period (Fig. 1B).

We next analyzed whole body energy homeostasis in these mice fed the same high fat diet using indirect calorimetry. Interestingly, despite the absence of a key enzyme in mitochondrial β-oxidation, $VLCAD^{-/-}$ mice had relatively higher percentage of fatty acid oxidation compared to WT controls reflected by a 20% decrease in RQ (calculated from area under the curves of Figure 1C, $P<0.01$). Overall energy expenditure was 15% lower (calculated from area under the curves of Figure 1D, $P<0.05$) in the $VLCAD^{-/-}$ mice. Measurements of intestinal fat absorption in $VLCAD^{-/-}$ and WT mice demonstrated no differences in fat absorption between the two groups when fed the same high fat diet (Table 1).

Taken together these data suggest that the $VLCAD^{-/-}$ mice are resistant to high-fat diet induced obesity due to decreased food intake. Since previous studies with carnitine palmitoyltransferase-1 inhibition in the hypothalamus have implicated increased hypothalamic long-chain acyl-CoA concentrations in reducing food intake (Obici et al., 2003) we examined hypothalamic long-chain acyl-CoA concentrations in fat fed $VLCAD^{-/-}$ and WT mice but found no differences in long-chain acyl-CoA concentrations (Table 1).

Since there was a marked difference in body weight between the two groups of mice after *ad lib* high-fat feeding, which is known to impact insulin stimulated glucose metabolism we subsequently studied VLCAD$^{-/-}$ and WT mice after 3 weeks of pair-feeding the high-fat diet. As expected, VLCAD$^{-/-}$ mice and WT mice pair-fed the high-fat diet had a similar body weight but VLCAD$^{-/-}$ mice had a 36% decrease in whole body fat content ($P<0.01$) as compared to WT control mice (Table 1). Basal plasma concentrations of glucose, insulin, triglyceride, β-hydroxybutyrate and cholesterol were similar in the two groups. However, plasma fatty acid levels were 30% higher in the VLCAD$^{-/-}$ mice consistent with their inborn error of metabolism as compared to the WT control mice. There were no differences in plasma concentrations of IL-6, TNFα or resistin between the two groups of mice (Table 1). However, adiponectin and leptin concentrations were both 40% lower in the VLCAD$^{-/-}$ mice compared to the WT controls.

VLCAD$^{-/-}$ mice were protected from high-fat diet induced insulin resistance

To investigate the effect of VLCAD$^{-/-}$ deficiency on glucose metabolism, we performed hyperinsulinemic-euglycemic clamp studies on WT and VLCAD$^{-/-}$ mice pair-fed the high-fat diet for 3 weeks. Reduced food intake in the WT mice (~450 kcal/kg/d) due to pair-feeding, as compared to their *ad lib* intake, did not protect the mice from severe insulin resistance caused by high-fat feeding (Fig. 2A). In stark contrast, VLCAD$^{-/-}$ mice required a significantly higher glucose infusion rate (Fig. 2A) in order to maintain euglycemia during the clamp reflecting increased whole body insulin sensitivity (Fig. 2B). This increased whole body insulin responsiveness in the VLCAD$^{-/-}$ mice could be attributed to both increased peripheral glucose uptake (Fig. 2B) and increased suppression of hepatic glucose production during the clamp (Fig. 2C). Consistent with these data VLCAD$^{-/-}$ mice also had significantly higher insulin stimulated 2-deoxy glucose uptake in skeletal muscle (Fig. 2D) during the clamp compared to the WT mice.

Consistent with the increased insulin suppression of hepatic glucose production in liver and insulin stimulated glucose uptake in muscle, insulin stimulated Akt2 activities in the liver and muscle of the VLCAD$^{-/-}$ mice were increased by 50% and 120%, respectively, compared to the WT controls (Figs. 2E and F). These data suggest that the VLCAD$^{-/-}$ mice are protected from high-fat diet induced insulin resistance both in liver and in skeletal muscle. This was further supported by glucose tolerance testing, with a significantly lower plasma glucose levels (Fig. 2G) and a trend of lower plasma insulin levels measured during the test (Fig. 2H).

Liver protein kinase Cε and muscle protein kinase Cθ activity are decreased in VLCAD$^{-/-}$ mice along with reduced intracellular diacylglycerol content

To determine if decreased activation of protein kinase Cε in liver and protein kinase Cθ in skeletal muscle played a role in protecting VLCAD$^{-/-}$ from fat induced insulin resistance we next measured protein kinase Cε and protein kinase Cθ activity in these tissues as reflected by the membrane to cytosol ratio of these proteins. Consistent with this hypothesis we found that protein kinase Cε and protein kinase Cθ activity were reduced by 35% and 50% respectively in the VLCAD$^{-/-}$ mice compared to the WT mice (Fig. 3A). Diacylglycerol (DAG) is a known activator of the novel PKCs and VLCAD$^{-/-}$ mice had less intracellular diacylglycerol (DAG) and triglyceride (TG) content compared to the WT mice (Figs. 3B and C). Acyl-CoA concentrations were significantly higher ($P<0.01$ [liver] and $P< 0.05$ [muscle]) in the VLCAD$^{-/-}$ mice as compared to the WT mice (Fig. 3D); however, ceramide, another putative mediator of fat induced insulin resistance, was not different in either liver or skeletal muscle in the two groups (Fig. 3E).

AMPK was activated in VLCAD−/− mice fed a high-fat diet

We found a 220% increase in liver and a 100% increase in muscle in AMPK activity in the VLCAD$^{-/-}$ mice compared to WT controls (Fig. 4A). We hypothesized that AMPK activation due to excess long-chain fatty acids in these tissues (Clark et al., 2004; Za'tara, et al., 2008) might explain the increased AMPK activity and serve as a compensatory mechanism to increase fat oxidation with a reduction in substrate available for DAG synthesis. The AMPK downstream target, acetyl-CoA carboxylase (ACC), was found to be phosphorylated 3 and 4 fold higher in the liver and muscle of the VLCAD$^{-/-}$ mice (Figs. 4C and D). Consistent with increased ACC phosphorylation, which leads to decreased ACC activity, liver malonyl-CoA content was also found to be lower in the VLCAD$^{-/-}$ mice (Fig. 3F). In contrast, there were no differences in liver or muscle AMPK activity in the LCAD deficient mice (Fig. 4B). In vitro measurements with freshly isolated liver, muscle and brown adipose tissue showed significantly higher rates of fatty acid oxidation in the VLCAD$^{-/-}$ mice compared to WT control mice (Fig. 4E). These data suggest that increased long-chain fatty acyl-CoAs (Fig. 3G) in the VLCAD−/− mice were able to activate AMPK and compensate partially for the loss of function in fatty acid oxidation, while significantly increasing insulin sensitivity in these mice. In contrast, however, the deficiency of fatty acid oxidation in the LCAD$^{-/-}$ mice did not lead to activation of AMPK (Fig. 4B) in liver or muscle, thus there was no compensation in fatty acid oxidation resulting in exacerbated hepatic insulin resistance in these mice (Zhang. et al., 2007). The predominant substrates that build up in LCAD deficiency are the medium-chain length $C_{14:1}$ acyl-CoA and $C_{14:1}$ acylcarnitine (Kurtz, et al, 1998; Zhang, et al., 2007).

We then measured acylcarnitines in plasma, muscle and liver of these mice since acylcarnitine measurement is an important clinical indicator for disorders in fatty acid oxidation. Plasma long chain acylcarnitines (C14 to C18) were slightly increased, however, liver and muscle long chain acylcarnitines were not statistically different (Supplemental Fig. 2).

In order to further understand the metabolic phenotype in these mice, we performed quantitative RT-PCR to measure liver, muscle and brown adipose tissue expression of genes involved in fatty acid metabolism in the WT and VLCAD$^{-/-}$ mice pair-fed high-fat diet. We found a dramatic compensatory increase in muscle and brown adipose tissue gene expression of PPARα and LCAD in the VLCAD$^{-/-}$ mouse group (Table 2). There was no difference in liver gene expression of PPARα and LCAD, probably because these genes in WT mice were also up regulated in liver due to high fat feeding. In addition, there was no difference in gene expression of PGC1α, PPARδ and AOX in liver, muscle or brown adipose tissue. Interestingly, muscle PGC1β and SREBP1 gene expression was down regulated significantly, indicating a strong transcriptional mechanism that reduces lipogenesis in skeletal muscle in the VLCAD$^{-/-}$ mice. In contrast, PGC1β and SREBP1 gene expression in liver and brown adipose tissue were not different. In addition, there was a 23% increase in UCP1 gene expression in brown adipose tissue of the VLCAD$^{-/-}$ mice.

Discussion

Characteristics of VLCAD deficiency in humans and mice

VLCAD deficiency is a potentially fatal disease, which frequently appears in the neonatal period presenting with hypoketotic/hypoglycemia, fatty liver, and cardiac disease (Roe and Ding, 2001). In direct side-by-side comparisons of the LCAD and VLCAD deficient mice (Cox, *et al*. 2001), we found many similarities with the other VLCAD$^{-/-}$ model (Exil, *et al*., 2003); however, we also found that the VLCAD deficient phenotype related to fatty acid oxidation deficiency is distinctly much milder than the LCAD deficient mice. This is further

borne out in a recent study (Cox, et al, 2009) that demonstrated a profound cardiac hypertrophy in the LCAD$^{-/-}$ males; whereas, the VLCAD$^{-/-}$ males had a very mild hypertrophy (Cox KB, et al., 2009). As described previously, the LCAD deficient mouse model (Kurtz, et al., 1998) is an excellent model of fatty acid oxidation deficiency for studying human VLCAD deficiency, as it has markedly elevated $C_{14:1}$ acylcarnitine, the hallmark acylcarnitine signature in human VLCAD deficiency; whereas, the VLCAD mouse models demonstrated a predominantly increased concentration of C_{16} and C_{18} acylcarnitines (Cox, et al, 2001; Spiekerkoetter, et al, 2004; Spiekerkoetter, et al, 2005), which are the acylcarnitines found at lower concentrations in WT mice. Furthermore, at least regarding the VLCAD deficient model (Cox, et al., 2001) used in the present studies, and in the previous studies when fed a standard rodent diet, the heart, liver and skeletal muscle had a normal level of palmitate oxidation despite there being no detectable VLCAD mRNA or protein, thus it appears that mouse LCAD activity for the most part compensates for VLCAD deficiency.

Insulin sensitivity and resistance to high-fat diet induced obesity in VLCAD$^{-/-}$ mice

VLCAD$^{-/-}$ mice had better glucose tolerance in response to a glucose tolerance test and were protected from developing high fat diet-induced insulin resistance as found in the WT control group. Interestingly, even though plasma fatty acids were higher in the VLCAD$^{-/-}$ mice, as is characteristic of their inherited enzyme deficiency, they were more insulin sensitive than the WT controls, thus disassociating insulin sensitivity from plasma fatty acid concentrations.

To investigate whether protection from diet-induced obesity in the VLCAD$^{-/-}$ mice was due to downstream effects of VLCAD deficiency and hypothalamic control of feeding behavior due to increased long chain acyl-CoAs as suggested by Obici and colleagues (Obici *et al*., 2003), we measured acyl-CoAs in the hypothalamus and found no significant differences between the genotypes. Furthermore, we found no differences in digestive fat absorption. We also evaluated fat utilization and energy expenditure. Surprisingly, we found a higher percentage of fat oxidation as reflected in the lower respiratory quotient (RQ) values in the VLCAD$^{-/-}$ mice as compared to the WT controls.

VLCAD$^{-/-}$ mice were resistant to developing whole body insulin resistance as reflected by a higher glucose infusion rate required to maintain euglycemia during the hyperinsulinemic-euglycemic clamp compared to the WT control mice. This increased whole body insulin responsiveness could be attributed to both increased insulin-stimulated skeletal muscle glucose uptake and increased insulin-stimulated suppression of hepatic glucose production in the VLCAD$^{-/-}$ mice compared to the pair fed WT control mice. This increased insulin action in liver and muscle could in turn be attributed to increased activation of Akt2 in both of these tissues. The increased insulin sensitivity was commensurate with decreased PKCε and PKCθ activity in liver and skeletal muscle respectively associated with decreased liver and muscle DAG and triglyceride concentrations in the VLCAD$^{-/-}$ mice. Increases in tissue ceramide content have been implicated in fat-induced insulin resistance (Holland *et al*., 2007) however in contrast to the increase in liver and muscle DAG concentrations of insulin resistant WT mice, there were no differences in liver or skeletal muscle ceramide concentrations between the VLCAD$^{-/-}$ and WT mice.

Activation of AMPK in VLCAD$^{-/-}$ mice

We found a significant elevation in AMPK activity in both liver and muscle of the VLCAD$^{-/-}$ mice as compared to WT control mice. We hypothesize that in mouse VLCAD deficiency AMPK is activated by elevated long-chain fatty acids (Table 1), as previously described (Clark *et al*., 2004; Za'tara, *et al*., 2008). The net effect of increased AMPK

activity was increased phosphorylation and inactivation of acetyl-CoA carboxylase in both liver and muscle, and this resulted in a significant reduction in malonyl-CoA in liver and a similar trend in muscle (data not shown). The resulting change in fat metabolism would be increased fatty acid oxidation (Fig. 4E), via LCAD activity as an alternative step to the deficient VLCAD step, resulting in a net reduction of DAG, which has been implicated in the pathogenesis of muscle and liver insulin resistance (Yu *et al*. 2002, Samuel *et al*. 2004).

Regulation of metabolic gene transcription in the VLCAD$^{-/-}$ mice

Previous studies have shown compensatory up regulation of PPARα activity on its target genes in response to a deficiency of the peroxisomal fatty acid oxidation enzyme acyl-CoA oxidase (AOX) (Fan *et al*., 1998). Likewise, we found significant increased expression of genes in the mitochondrial fatty acid oxidation pathway in the VLCAD$^{-/-}$ mice including genes for PPARα and LCAD in both skeletal muscle and brown adipose tissue (BAT) (Table 2). There were no differences in gene expression of PPARδ in liver, muscle or brown adipose tissue in the VLCAD$^{-/-}$ mice compared to the WT mice, suggesting that PPARα activated mitochondrial fatty acid oxidation in muscle and BAT of the VLCAD$^{-/-}$ mice is a compensatory mechanism to increase energy production in these tissues. In addition, we found an approximately 25% increase in UCP1 and peroxisomal AOX gene expression in BAT of the VLCAD$^{-/-}$ mice, which would also promote increased fat oxidation and energy dissipation.

In summary, we found that VLCAD$^{-/-}$ mice, when challenged by a high-fat diet, were significantly resistant to developing insulin resistance as compared with WT control mice fed the same diet. The pivotal changes that likely explain these results include a significantly increased rate of fatty acid oxidation rate due to both increased PPARα stimulation of peroxisomal fatty acid oxidation gene expression and increased AMPK activity in liver and muscle that would reduce malonyl-CoA suppression of fatty acid oxidation, as well as reduce substrate for endogenous fatty acid synthesis. The net result was significantly reduced DAG concentrations in liver and skeletal muscle commensurate with reduced PKCε and PKCθ activity respectively, which have been shown to cause insulin resistance in these tissues (Griffin *et al*., 1999; Yu *et al*., 2002; Samuel *et al*. 2004, Neschen *et al*., 2005, Savage *et al*. 2006, Samuel *et al*. 2007) (Fig. 5). Taken together these studies support the hypothesis that fat-induced insulin resistance is due to an imbalance of fatty acid delivery/synthesis versus mitochondrial/peroxisomal fatty acid oxidation and that reductions in specific steps, such as VLCAD, mitochondrial fatty acid oxidation as observed in the VLCAD$^{-/-}$ mice and other mouse models (Wredenberg et al., 2006; Pospisilik et al., 2007) can promote increased insulin-stimulated glucose metabolism by compensatory mechanisms involving activation of AMPK and PPARα.

Materials and Methods

Animals

Male VLCAD$^{-/-}$, LCAD$^{-/-}$ and WT controls were produced as described previously (Cox et al., 2001) and studied at approximately 12 weeks of age. VLCAD$^{-/-}$ and WT mice had a 129S6/B6 mixed background. Animals were housed under controlled temperature (23°C) and lighting (12 hours of light and 12 hours of dark) with free access to water and standard rodent diet (Harlan Teklad 2018S). All mice were fasted for 6 hours starting at 8 am before experiments. Body composition measurements were performed on awake mice using Bruker Mini-spec Analyzer (Bruker, TX). To examine the diet-induced changes in glucose and fat metabolism, male VLCAD$^{-/-}$, LCAD$^{-/-}$ and WT mice were fed a regular diet (TD2018; Harlan Teklad, Madison, WI) or HFD (55% fat by calories; TD 93075; Harlan Teklad) ad libitum at the age of 17–18 weeks for 3 weeks, and metabolic parameters and insulin action

were measured. For glucose tolerance test, 1 g glucose/kg was introduced intraperitoneally for each mouse with blood samples collected at indicated time intervals from the tail tips.

A comprehensive animal metabolic monitoring system (CLAMS; Columbus Instruments, Columbus, OH) was used to evaluate RQ and energy expenditure in mice after 3 weeks of high-fat pair feeding. Energy expenditure data were normalized with respect to lean body weight. Energy expenditure and RQ were calculated from the gas exchange data [energy expenditure = (3.815 + 1.232 × RQ) × VO2]. RQ is the ratio of VCO_2 to VO_2, which changes depending on the energy source the animal is using. When carbohydrates are the only substrate being oxidized, the RQ will be 1.0, and it will be 0.7 when only fatty acids are oxidized. We studied five to eight male mice per group. All procedures were approved by the University of Alabama at Birmingham and the Yale University Animal Care and Use Committees.

Hyperinsulinemic-euglycemic clamp

At least 4 days before hyperinsulinemic-euglycemic clamp experiments, mice were anesthetized with an intraperitoneal injection of ketamine (100 mg/kg body weight) and xylazine (10 mg/kg body weight), and an indwelling catheter was inserted in the left internal jugular vein. The catheters were externalized through an incision in the skin flap behind the head, and the mice were returned to individual cages after the surgery. To conduct experiments in awake mice with minimal stress, a tail restraint method was used (Kim et al., 2000). A 120-min hyperinsulinemic-euglycemic clamp was conducted with a prime-continuous infusion of human insulin (Humulin, Eli Lilly) at a rate of 2.5 mU/kg/min (15 pmol/kg/min) to raise plasma insulin levels. Blood samples (20 μl) were collected at 20 min intervals for the immediate measurement of plasma glucose concentration, and 20% glucose was infused at variable rates to maintain plasma glucose at basal concentrations. Insulin-stimulated whole-body glucose flux was estimated using a prime-continuous infusion of [3-^{3}H] glucose (10 μCi bolus, 0.1 μCi/min; NEN Life Science Products Inc.) throughout the clamps. All infusions were done using microdialysis pumps (CMA/Microdialysis, North Chelmsford, Massachusetts, USA). To estimate insulin-stimulated glucose uptake and metabolism in individual tissues, 2-[^{14}C]-deoxyglucose (NEN Life Science Products Inc.) was administered as a bolus (10 μCi) at 75 minutes after the start of clamps. Blood samples (20 μl) were taken at 80, 85, 90, 100, 110, and 120 minutes after the start of clamps for the determination of plasma [^{3}H]glucose, ^3H_2O, and 2-[^{14}C]-deoxyglucose concentrations. Additional blood samples were obtained before the start and at the end of clamps for measurement of plasma insulin and free fatty acid concentrations. At the end of clamps, mice were anesthetized with sodium pentobarbital overdose. Within 5 minutes, four muscles (soleus, gastrocnemius, tibialis anterior, and quadriceps) from both hind limbs, epididymal white adipose tissue, intrascapular brown adipose tissue and liver were taken. Each tissue, once exposed, was dissected out within 2 seconds, frozen immediately using liquid N_2-cooled aluminum blocks, and stored at −70°C for later analysis.

Calculations

Rates of basal endogenous glucose production and insulin-stimulated whole-body glucose uptake were determined as the ratio of the [^{3}H]glucose infusion rate (disintegrations per minute [dpm]/min) to the specific activity of plasma glucose (dpm/μmol) during the final 30 minutes of basal and clamp periods, respectively. Endogenous glucose production during clamps was determined by subtracting the glucose infusion rate from the whole-body glucose uptake (Rossetti et al., 1990). Glucose uptake in individual tissues was calculated from plasma 2-[^{14}C]-deoxyglucose profile, which was fitted with a double exponential curve using MLAB (Civilized Software, Bethesda, Maryland, USA) and tissue 2-deoxyglucose-6-phosphate content as described previously (Kim et al., 1996).

Biochemical Assays

Plasma glucose concentrations during clamps were measured using 10 μl plasma by a glucose oxidase method on a Beckman glucose analyzer II (Beckman Instruments Inc., Fullerton, California, USA), and plasma insulin concentrations were measured by RIA using kits from Linco Research Inc. (St. Charles, Missouri, USA). Plasma fatty acid concentrations were determined using an acyl-CoA oxidase-based colorimetric kit (Wako Chemicals USA Inc., Richmond, Virginia, USA). Fat absorption in the gut was measured according to (Jandacek et al., 2004). For the determination of plasma [3-^{3}H]glucose and 2-[^{14}C]-deoxyglucose concentrations, plasma was deproteinized with $ZnSO_4$ and $Ba(OH)_2$, dried to remove $^{3}H_2O$, resuspended in water, and counted in scintillation fluid (Ultima Gold; Packard Instrument Co., Meriden, Connecticut) on dual channels for separation of ^{3}H and ^{14}C. The plasma concentration of $^{3}H_2O$ was determined by the difference between ^{3}H counts without and with drying. For the determination of tissue 2-[^{14}C]-deoxyglucose-6-phosphate content, tissue samples were homogenized, and the supernatants were subjected to an ion-exchange column to separate 2-deoxyglucose-6-phosphate from 2-deoxyglucose, as described previously (Kim et al., 2000). Skeletal muscle and liver triglyceride concentrations were determined using triglyceride assay kit (Sigma Chemical Co.) and a method adapted from (Storlien et al., 1991). Long-chain acyl-CoA and diacylglycerol concentrations in skeletal muscle and liver were measured as previously described (Yu et al., 2002). Akt2 (Alessi et al., 1996), AMPK (Reznick et al., 2007) and PKCε (Samuel et al., 2004) assays were performed as previously described. For in vitro tissue fatty acid oxidation analysis, the liver, gastrocnemius muscle and brown adipose tissue were removed from anesthetized mice just prior to sacrifice. Approximately 115 mg of tissue were immediately placed in 1 mL of homogenization buffer (250 mM sucrose, 1 mM EDTA, and 10 mM tris-HCl, pH 7.4) on ice. After mincing with scissors, the tissues were homogenized in a Kontes duall 21 glass homogenizer for 15 passes across 30 sec at 800 RPM with a motor driven Teflon pestle. The homogenates were then flushed with 95% oxygen/5% CO_2 for 15 minutes on ice. The palmitate oxidation was then determined by adding 600 uL of the homogenate to 2.65 mL of reaction mixture (100 mM sucrose, 10 mM Tris-HCl, 5 mM potassium phosphate, 80 mM potassium chloride, 1 mM magnesium chloride, 2 mM L-carnitine, 0.1 mM malate, 2 mM ATP, 0.05 mM coenzyme A, 1 mM dithiothreitol, 0.2 mM EDTA, 0.5 uCi 1-^{14}C-Palmitate, and 0.3% bovine serum albumin), sealing the flasks immediately with kontes rubber stoppers, and lightly shaking the mixture for 60 minutes in a 30°C water bath. The CO_2 in the reaction mixture was then liberated by the addition 300 uL of 12 M HCL and trapped with whatman paper soaked with 300 uL of 2 M sodium hydroxide. The trapped $^{14}CO_2$ was then measured by liquid scintillation counting using a Perkin Elmer Tri-Carb 3100TR scintillation counter (Doh et al., 2005).

Quantitative RT-PCR-based Gene Expression

RNA was isolated from tissues using a commercially available kit (Qiagen RNeasy Kit, Qiagen Inc, Valencia, CA) in combination with DNase I treatment. After 2 μg of total RNA were reverse transcribed (Stratagene, La Jolla, CA) with random primers, quantitative PCR was performed with a DNA Engine Opticon 2 System (MJ Research, Boston, MA) using SYBR green QPCR dye kit (Stratagene, La Jolla, CA). The following primers were used: PPARα: 5′-GCAGCTCGTACAGGTCATCA-3′ (F) and 5′-CTCTTCATCCCCAAGCGTAG-3′ (R); PPARδ: 5′- CTGAAGGGAAGGGGGTAGAG-3′ (F) and 5′-TTCCTGGTACTGGGATCTGC-3′ (R); PPARγ: 5′-ATGCCAAAAATATCCCTGGTTTC-3′ (F) and 5′-GGAGGCCAGCATGGTGTAGA-3′ (R); MCAD: 5′-GCATCAACATCGCAGAGAAA-3′ (F) and 5′-CATTGTCCAAAAGCCAAACC-3′ (R); LCAD: 5′- GCATCAACATCGCAGAGAAA-3′ (F) and 5′-GGCTATGGCACCGATACACT-3′ (R); CPT1a: 5′-AACCCAGTGCCTTAACGATG-3′ (F) and 5′- GAACTGGTGGCCAATGAGAT-3′ (R);

CPT1b: 5′- TTGTGCAGATTGCCCTACAG-3′ (F) and 5′-GTCATGGCTAGGCGGTACAT-3′ (R); CPT2: 5′- GAAGAAGCTGAGCCCTGATG-3′ (F) and 5′- GCCATGGTATTTGGAGCACT-3′ (R); AOX: 5′-AGCTCCGATCAGCCAGACAT-3′ (F) and 5′-TTCTTGAAACAGAGCCCAGAATG-3′ (R); SREBP1: 5′-CAGCTCAGAGCCGTGGTGA-3′ (F) and 5′-TTGATAGAAGACCGGTAGCGC-3′ (R); CHREBP: 5′-ACCTGTCTCCCCCTCAAACT-3′ (F) and 5′-TGTCTTCTGAAGCGTGGTTG-3′ (R); PGC1α: 5′-ATGTGTCGCCTTCTTGCTCT-3′ (F) and 5′-ATCTACTGCCTGGGGACCTT-3′ (R); PGC1β: 5′- AACCCAACCAGTCTCACAGG-3′ (F) and 5′-CTCCTAGGGGCCTTTGTTTC-3′ (R); SCD1: 5′-AGATCTCCAGTTCTTACACGACCAC-3′ (F) and 5′-GACGGATGTCTTCTTCCAGGTG-3′ (R); ACC1: 5′- ATTGGGCACCCC AGAGCTA-3′ (F) and 5′- CCCGCTCCTTCAACTTGCT-3′ (R); ACC2: 5′-GGGCTCCCTGGATGACAAC-3′ (F) and 5′- TTCCGGGAGGAGTTCTGGA-3′ (R); DGAT1: 5′- GTTCCGCCTCTGGGCATT-3′ (F) and 5′-GAATCGGCCCACAATCCA-3′ (R); DGAT2: 5′- ACTCTGGAGGTTGGCACCAT-3′ (F) and 5′-GGGTGTGGCTCAGGAGGAT-3′ (R); LXRα: 5′- AGCGTCCATTCAGAGCAAGT-3′ (F) and 5′- CCCTTCTCAGTCTGCTCCAC-3′ (R); CYP7A1: 5′-GGTCCTCCAGCAGAGAGCTA-3′ (F) and 5′- TTGCTTAAGCTACGCGGAAT-3′ (R); FXR: 5′- AAAAGGGGATGAGCTGTGTG-3′ (F) and 5′-ACATCCCCATCTCTCTGCAC-3′ (R); ABCB11: 5′-GGCTTGCTACAGATGCTTCC-3′ (F) and 5′- GCCAAAAAGGGGAAGAAGAC-3′ (R); UCP1: 5′-GGGCCCTTGTAAACAACAAA-3′ (F) and 5′- GTCGGTCCTTCCTTGGTGTA-3′ (R); UCP2: 5′- GTAGCACCCGACCTCTGAAG-3′ (F) and 5′-ATGGGTCGTGGAGACTTGAC-3′ (R); UCP3: 5′-TGCTGAGATGGTGACCTACG-3′ (F) and 5′- GCGTTCATGTATCGGGTCTT-3′ (R); 18S rRNA: 5′-TTC CGA TAA CGA ACG AGA CTC T-3′ (F) and 5′-TGGCTGAACGCCACTTGTC-3′ (R). Product specificity was verified by running products on an agarose gel. Messenger RNA levels (ΔC_T values), normalized to 18S rRNA were expressed using the comparative method. 18S rRNA levels showed no statistical difference between genotypes.

Statistical analysis

Data are expressed as means ± standard error. The significance of the differences in mean values between WT and VLCAD$^{-/-}$, LCAD$^{-/-}$ mice were evaluated by using the unpaired Student's *t* test.

Supplementary Material

Refer to Web version on PubMed Central for supplementary material.

Acknowledgments

We thank Aida Grosmann, Takamasa Higashimori, Hyo-Jeong Kim, You-Ree Cho and Doug Hamm for their technical assistance. This project was supported by grants from the United States Public Health Service: R01 RR-02599 (PAW) R01 DK-40936 (GIS), U24 DK-59635 (GIS) and a Distinguished Clinical Scientist Award from the American Diabetes Association (GIS). The paper's contents are solely the responsibility of the authors and do not necessarily represent the official views of NCRR, NIDDK or NIH.

References

Alessi DR, Caudwell FB, Andjelkovic M, Hemmings BA, Cohen P. Molecular basis for the substrate specificity of protein kinase B; comparison with MAPKAP kinase-1 and p70 S6 kinase. FEBS Lett. 1996; 399:333–338. [PubMed: 8985174]

Clark H, Carling D, Saggerson D. Covalent activation of heart AMP-activated protein kinase in response to physiological concentrations of long-chain fatty acids. Eur J Biochem. 2004; 271:2215–2224. [PubMed: 15153111]

Cox KB, Hamm DA, Millington DS, Matern D, Vockley J, Rinaldo P, Pinkert CA, Rhead WJ, Lindsey JR, Wood PA. Gestational, pathologic and biochemical differences between very long-chain acyl-CoA dehydrogenase deficiency and long-chain acyl-CoA dehydrogenase deficiency in the mouse. Hum. Mol. Genet. 2001; 10:2069–2077. [PubMed: 11590124]

Cox KB, Liu J, Tian L, Barnes S, Yang Q, Wood PA. Cardiac hypertrophy in mice with long-chain acyl-CoA dehydrogenase or very long-chain acyl-CoA dehydrogenase deficiency. Lab. Invest. 2009; 89:1348–1354. [PubMed: 19736549]

Doh KO, Kim YW, Park SY, Lee SK, Park JS, Kim JY. Interrelation between long-chain fatty acid oxidation rate and carnitine palmitoyltransferase 1 activity with different isoforms in rat tissues. Life Sci. 2005; 77:435–43. [PubMed: 15894012]

Exil VJ, Roberts RL, Sims H, McLaughlin JE, Malkin RA, Gardner CD, Ni G, Rottman JN, Strauss AW. Very-long-chain acyl-coenzyme a dehydrogenase deficiency in mice. Circ Res. 2003; 93:448–455. [PubMed: 12893739]

Fan CY, Pan J, Usuda N, Yeldandi AV, Rao MS, Reddy JK. Steatohepatitis, spontaneous peroxisome proliferation and liver tumors in mice lacking peroxisomal fatty acyl-CoA oxidase. Implications for peroxisome proliferator-activated receptor alpha natural ligand metabolism. J. Biol. Chem. 1998; 273:15639–45. [PubMed: 9624157]

Griffin ME, Marcucci MJ, Cline GW, Bell K, Barucci N, Lee D, Goodyear LJ, Kraegen EW, White MF, Shulman GI. Free fatty acid-induced insulin resistance is associated with activation of protein kinase C theta and alterations in the insulin signaling cascade. Diabetes. 1999; 48:1270–4. [PubMed: 10342815]

Holland WL, Brozinick JT, Wang LP, Hawkins ED, Sargent KM, Liu Y, Narra K, Hoehn KL, Knotts TA, Siesky A, Nelson DH, Karathanasis SK, Fontenot GK, Birnbaum MJ, Summers SA. Inhibition of ceramide synthesis ameliorates glucocorticoid-, saturated-fat-, and obesity-induced insulin resistance. Cell Metab. 2007; 5:167–79. [PubMed: 17339025]

Jandacek RJ, Heubi JE, Tso P. A novel, noninvasive method for the measurement of intestinal fat absorption. Gastroenterology. 2004; 127:139–44. [PubMed: 15236180]

Kelley DE, He J, Menshikova EV, Ritov VB. Dysfunction of mitochondria in human skeletal muscle in type 2 diabetes. Diabetes. 2002; 51:2944–2950. [PubMed: 12351431]

Kim JK, Wi JK, Youn JH. Plasma free fatty acids decrease insulin-stimulated skeletal muscle glucose uptake by suppressing glycolysis in conscious rats. Diabetes. 1996; 45:446–453. [PubMed: 8603766]

Kim JK, Gavrilova O, Chen Y, Reitman ML, Shulman GI. Mechanism of insulin resistance in A-ZIP/F-1 fatless mice. J. Biol. Chem. 2000; 275:8456–8460. [PubMed: 10722680]

Lee SS, Pineau T, Drago J, Lee EJ, Owens JW, Kroetz DL, Fernandez-Salguero PM, Westphal H, Gonzalez FJ. Targeted disruption of the alpha isoform of the peroxisome proliferator-activated receptor gene in mice results in abolishment of the pleiotropic effects of peroxisome proliferators. Mol. Cell. Biol. 1995; 15:3012–22. [PubMed: 7539101]

Mootha VK, Bunkenborg J, Olsen JV, Hjerrild M, Wisniewski JR, Stahl E, Bolouri MS, Ray HN, Sihag S, Kamal M, Patterson N, Lander ES, Mann M. Integrated analysis of protein composition, tissue diversity, and gene regulation in mouse mitochondria. Cell. 2003; 115:629–40. [PubMed: 14651853]

Neschen S, Morino K, Hammond LE, Zhang D, Liu ZX, Romanelli AJ, Cline GW, Pongratz RL, Zhang XM, Choi CS, Coleman RA, Shulman GI. Prevention of hepatic steatosis and hepatic insulin resistance in mitochondrial acyl-CoA:glycerol-sn-3-phosphate acyltransferase 1 knockout mice. Cell Metab. 2005; 2:55–65. [PubMed: 16054099]

Obici S, Feng Z, Arduini A, Conti R, Rossetti L. Inhibition of hypothalamic carnitine palmitoyltransferase-1 decreases food intake and glucose production. Nat. Med. 2003; 9:756–61. [PubMed: 12754501]

Patti ME, Butte AJ, Crunkhorn S, Cusi K, Berria R, Kashyap S, Miyazaki Y, Kohane I, Costello M, Saccone R, Landaker EJ, Goldfine AB, Mun E, DeFronzo R, Finlayson J, Kahn CR, Mandarino

LJ. Coordinated reduction of genes of oxidative metabolism in humans with insulin resistance and diabetes: Potential role of PGC1 and NRF1. Proc. Natl. Acad. Sci. U.S.A. 2003; 100:8466–71. [PubMed: 12832613]

Petersen KF, Befroy D, Dufour S, Dziura J, Ariyan C, Rothman DL, DiPietro L, Cline GW, Shulman GI. Mitochondrial dysfunction in the elderly: possible role in insulin resistance. Science. 2003; 300:1140–1142. [PubMed: 12750520]

Petersen KF, Dufour S, Befroy D, Garcia R, Shulman GI. Impaired mitochondrial activity in the insulin-resistant offspring of patients with type 2 diabetes. N. Engl. J. Med. 2004; 350:664–671. [PubMed: 14960743]

Pospisilik JA, Knauf C, Joza N, Benit P, Orthofer M, Cani PD, Ebersberger I, Nakashima T, Sarao R, Neely G, Esterbauer H, Kozlov A, Kahn CR, Kroemer G, Rustin P, Burcelin R, Penninger JM. Targeted deletion of AIF decreases mitochondrial oxidative phosphorylation and protects from obesity and diabetes. Cell. 2007; 131:476–91. [PubMed: 17981116]

Reznick RM, Zong H, Li J, Morino K, Moore IK, Yu HJ, Liu ZX, Dong J, Mustard KJ, Hawley SA, Befroy D, Pypaert M, Hardie DG, Young LH, Shulman GI. Aging-associated reductions in AMP-activated protein kinase activity and mitochondrial biogenesis. Cell Metab. 2007; 5:151–6. [PubMed: 17276357]

Roe, C.; Ding, J. Mitochondrial fatty acid oxidation disorders. In: Scriver, CR.; Beaudet, AL.; Sly, WS.; Valle, D.; Childs, B.; Kinzler, KW.; Vogelstein, B., editors. The Metabolic and Molecular Bases of Inherited Disease. McGraw-Hill; New York: 2001. p. 2297-2326.

Rossetti L, Giaccari A. Relative contribution of glycogen synthesis and glycolysis to insulin-mediated glucose uptake. A dose-response euglycemic clamp study in normal and diabetic rats. J. Clin. Invest. 1990; 85:1785–1792. [PubMed: 2189891]

Samuel VT, Liu ZX, Qu X, Elder BD, Bilz S, Befroy D, Romanelli AJ, Shulman GI. Mechanism of hepatic insulin resistance in non-alcoholic fatty liver disease. J. Biol. Chem. 2004; 279:32345–3253. [PubMed: 15166226]

Samuel V, Liu Z, Wang A, Beddow S, Geisler J, Kahn M, Zhang X, Monia B, Bhanot S, Shulman GI. Inhibition of Protein Kinase Cε Prevents Hepatic Insulin Resistance In Nonalcoholic Fatty Liver Disease. J Clin Invest. 2007; 117:739–745. [PubMed: 17318260]

Savage D, Choi C, Samuel V, Liu Z, Zhang D, Wang A, Zhang X, Cline G, Yu X, Geisler J, Bhanot S, Monia B, Shulman GI. Reversal of diet-induced hepatic steatosis and hepatic insulin resistance by antisense oligonucleotide inhibitors of acetyl-CoA carboxylase 1 and 2. J Clin Invest. 2006; 116:817–824. [PubMed: 16485039]

Spiekerkoetter U, Tokunaga C, Wendel U, Mayatepek E, Exil V, Duran M, Wijburg FA, Wanders RJ, Strauss AW. Changes in blood carnitine and acylcarnitine profiles of very long-chain acyl-CoA dehydrogenase-deficient mice subjected to stress. Eur J Clin Invest. 2004; 34:191–196. [PubMed: 15025677]

Spiekerkoetter U, Tokunaga C, Wendel U, Mayatepek E, Ijlst L, Vaz FM, van Vlies N, Overmars H, Duran M, Wijburg FA, Wanders RJ, Strauss AW. Tissue carnitine homeostasis in very-long-chain acyl-CoA dehydrogenase-deficient mice. Pediatr Res. 2005; 57:760–764. [PubMed: 15774826]

Storlien LH, Jenkins AB, Chisholm DJ, Pascoe WS, Khouri S, Kraegen EW. Influence of dietary fat composition on development of insulin resistance in rats. Relationship to muscle triglyceride and omega-3 fatty acids in muscle phospholipid. Diabetes. 1991; 40:280–289. [PubMed: 1991575]

Wredenberg A, Freyer C, Sandström ME, Katz A, Wibom R, Westerblad H, Larsson NG. Respiratory chain dysfunction in skeletal muscle does not cause insulin resistance. Biochem Biophys Res Commun. 2006; 350:202–7. [PubMed: 16996481]

Yu C, Chen Y, Cline GW, Zhang D, Zong H, Wang Y, Bergeron R, Kim JK, Cushman SW, Cooney GJ, Atcheson B, White MF, Kraegen EW, Shulman GI. Mechanism by which fatty acids inhibit insulin activation of insulin receptor substrate-1 (IRS-1)-associated phosphatidylinositol 3-kinase activity in muscle. J. Biol. Chem. 2002; 277:50230–50236. [PubMed: 12006582]

Za'tara G, Bar-Tana J, Kalderon B, Suter M, Morad E, Samovski D, Neumann D, Hertz R. AMPK activation by long chain fatty acyl analogs. Biochem Pharmacol. 2008; 76:1263–1275. [PubMed: 18812171]

Zhang D, Liu ZX, Choi CS, Tian L, Kibby R, Dong J, Cline GW, Wood PA, Shulman GI. Mitochondrial dysfunction due to long-chain Acyl-CoA dehydrogenase deficiency causes hepatic steatosis and hepatic insulin resistance. Proc. Natl. Acad. Sci. U.S.A. 2007; 104:17075–80. [PubMed: 17940018]

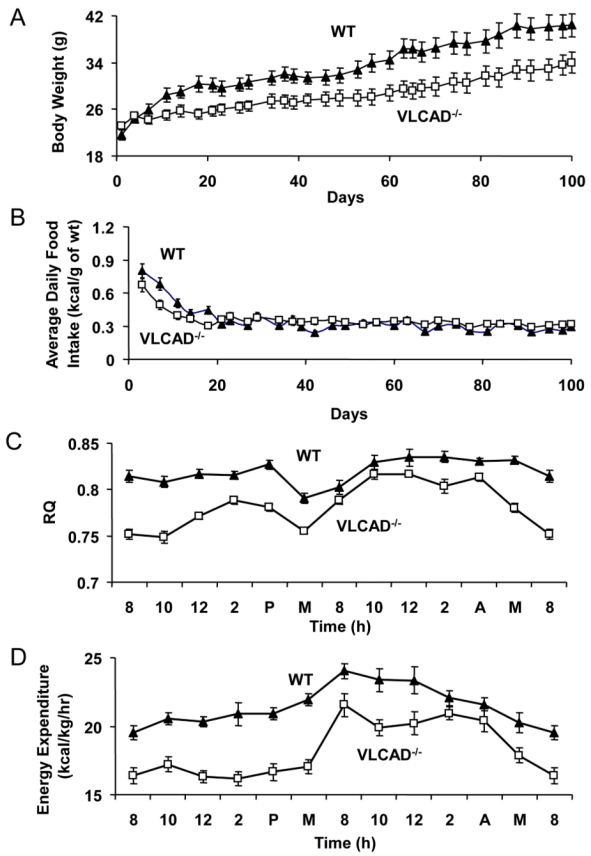

Figure 1.

(A) VLCAD$^{-/-}$ mice have significantly lower body weight ($P<0.05$) than WT mice when fed a high-fat diet ad lib for 100 days. (B) VLCAD$^{-/-}$ mice have significantly lower food intake ($P<0.05$) as compared to WT mice fed a high-fat diet ad lib for the first two weeks of feeding. (C) VLCAD$^{-/-}$ mice have significantly lower RQ ($P<0.001$) and (D) lower energy expenditure ($P<0.02$) as compared to WT controls measured over 24 hours. RQ and energy expenditure measurements were performed on mice pair-fed high-fat diet for 3 months. Both groups n=7. Values are mean ± SEM.

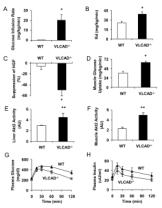

Figure 2.

VLCAD$^{-/-}$ mice are resistant to high-fat induced insulin resistance as demonstrated by (A) a significantly higher glucose infusion rate, (B) significantly higher whole body glucose uptake (Rd), (C) significantly higher insulin-mediated suppression of hepatic glucose production (HGP), and (D) a significantly higher skeletal muscle glucose uptake as compared to WT controls pair-fed high fat diet. The downstream effects include significantly increased Akt2 activity in the liver (E) and muscle (F) of VLCAD$^{-/-}$ mice. VLCAD$^{-/-}$ mice also had improved glucose tolerance during IPGTT, as shown by a significantly lower glucose curve (G) as compared to WT, while the insulin curve was also trending lower (H). *, $P<0.05$. **, $P<0.01$. Both groups n=7 and were pair-fed the high-fat diet. Values are mean± SEM.

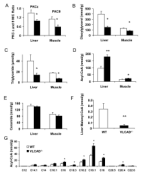

Figure 3.

(A) Protein kinase Cε or θ membrane translocation (activation) in liver and muscle of VLCAD$^{-/-}$ mice was significantly decreased as compared to WT controls; (B) diacylglycerol (DAG) and (C) triglyceride (TG) concentrations in liver were significantly lower in the VLCAD$^{-/-}$ mice; (D) VLCAD$^{-/-}$ mice had significantly higher total acyl-CoA concentrations in liver ($P< 0.01$) and muscle; (E) there were no significant differences in the liver ceramide concentrations; (F) Liver malonyl-CoA significantly lower in VLCAD$^{-/-}$ mice. (G) Liver acyl-CoA profile. Open bars are WT and black filled bars indicate VLCAD$^{-/-}$ mice. *, $P<0.05$. **, $P<0.01$. Both groups n=7 and were pair-fed the high-fat diet. Values are mean± SEM.

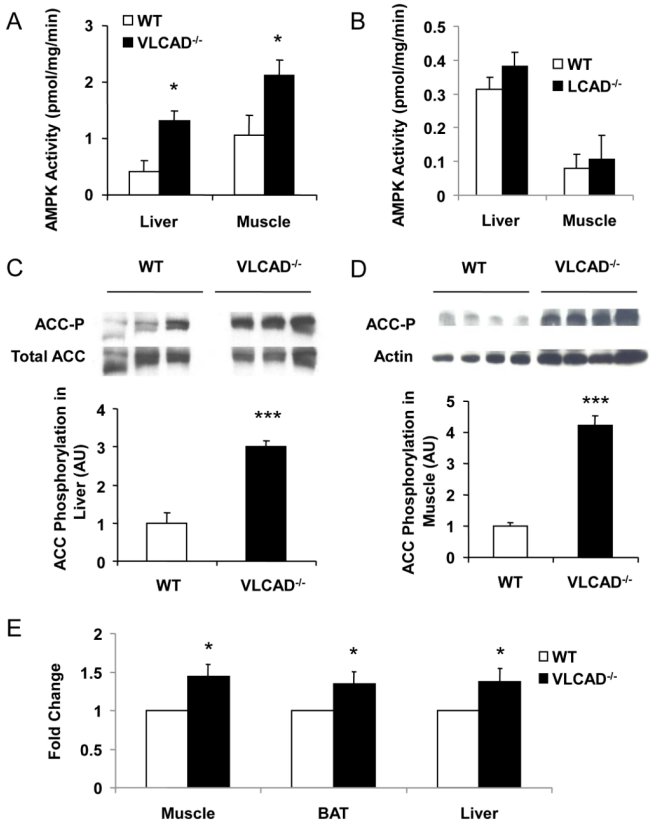

Figure 4.

AMPK activity and phospho-acetyl-CoA carboxylase. AMPK activity is significantly elevated in (A) VLCAD$^{-/-}$ liver and skeletal muscle; but not in (B) LCAD$^{-/-}$ liver and skeletal muscle; VLCAD$^{-/-}$ mice have significantly increased phosphorylated (inactivated form) ACC in both (C) liver and (D) skeletal muscle. (E) fatty acid oxidation is significantly increased in VLCAD$^{-/-}$ mouse liver, brown adipose tissue (BAT) and skeletal muscle. *, P<0.05. **, P<0.01. ***, P<0.001. All groups have n=7. Values are mean± SEM.

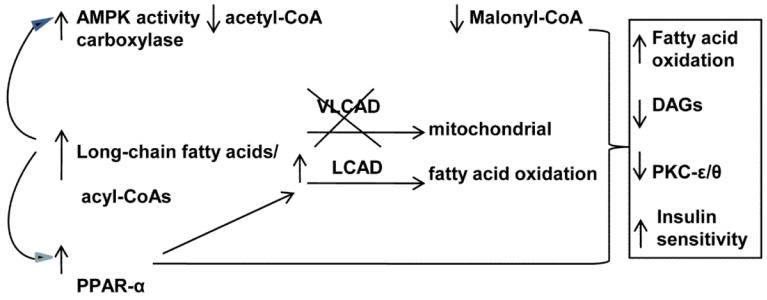

Figure 5.

Schematic summary of increased fatty acid oxidation and insulin sensitivity in high fat fed VLCAD$^{-/-}$ mice. We hypothesize that due to the build-up of long-chain fatty acids in the mouse VLCAD deficient state with enzymatic compensation provided by intact LCAD activity, there is a stimulation of fatty acid oxidation via (1) direct activation of AMPK and (2) stimulation of PPAR-α with the collective downstream activation of mitochondrial fatty acid oxidation. The net effect is a resistance in the VLCAD $^{-/-}$ mice to the build-up of DAG and the insulin resistant state found in the high-fat fed WT mice.

Table 1

Metabolic profile in plasma of the WT and VLCAD$^{-/-}$ mice pair-fed high-fat diet for 3 weeks

	WT	VLCAD$^{-/-}$
Body Weight (g)	28.3 ± 1.4	29.2 ± 0.5
Fat Mass (g)	4.7 ± 0.7	3.0 ± 0.2*
Glucose (mg/dl)	172 ± 7.3	168 ± 7.4
Insulin (pM)	167 ± 33	137 ± 16
Adiponectin (mg/ml)	7.9 ± 0.7	4.9 ± 0.5*
Leptin (ng/ml)	7.1 ± 1.3	3.8 ± 0.5*
IL-6 (pg/ml)	17 ± 3.6	28 ± 4.4
TNFα (pg/ml)	6.8 ± 1.6	9.3 ± 1.1
Resistin (ng/ml)	2.7 ± 0.4	2.1 ± 0.1
Triglyceride (mg/dl)	38 ± 2.5	41 ± 2.5
NEFA (mM)	0.62 ± 0.03	0.81 ± 0.03*
β-Hydroxybutyrate (mM)	0.33 ± 0.07	0.23 ± 0.04
Total Cholesterol (mg/dl)	64 ± 4.9	77 ± 7.6
Fat absorption (%)	99.0 ± 0.3	99.5 ± 0.1
Hypothalamus Acyl-CoA (nmol/g)	48.2 ± 3.8	51.7 ± 6.1

Fat mass and lean mass were obtained from awake mice with a Bruker Mini-spec Analyzer. Plasma glucose and insulin were basal values before the hyperinsulinemic-euglycemic clamp. Data represent mean ± SEM of 9 mice per group.

* $P < 0.01$ compared with wild type controls.

Table 2

Gene expression relative to 18S in the liver, muscle, and brown adipose tissue of high-fat fed WT and VLCAD$^{-/-}$ mice (×10^8)

	Fed Liver		Fasted Liver		Muscle		BAT	
	WT	**VLCAD$^{-/-}$**	**WT**	**VLCAD$^{-/-}$**	**WT**	**VLCAD$^{-/-}$**	**WT**	**VLCAD$^{-/-}$**
PPARα	126000 ± 19300	116000 ± 17600	344 ± 52	408 ± 47	5.8 ± 0.7	11 ± 1.4*	3420 ± 540	6250 ± 610*
PPARδ	3360 ± 864	1670 ± 149	316 ± 16	351 ± 41	4.6 ± 0.5	4.1 ± 0.6	1360 ± 66	1810 ± 250
PPARγ	2690 ± 357	2920 ± 249	3.2 ± 0.42	5.8 ± 0.98*	147 ± 29	125 ± 27	3280 ± 1290	2180 ± 548
MCAD	82100 ± 8560	92100 ± 1130	18200 ± 1780	52500 ± 1320*	149 ± 5	253 ± 32*	708000 ± 321000	432000 ± 64500
LCAD	317 ± 24	315 ± 34	294 ± 28	285 ± 48	208 ± 22	338 ± 42*	320000 ± 26300	448000 ± 47000*
CPT1	681 ± 63	644 ± 57	104000 ± 14600	158000 ± 27800	48 ± 2.6	55 ± 3.8	342 ± 160	273 ± 53
CPT2	39100 ± 5530	27000 ± 1260	5670 ± 497	10700 ± 1690*	18 ± 1.6	23 ± 1.6*	26300 ± 1630	26900 ± 1500
AOX			3593 ± 708	3789 ± 524	28 ± 3.3	30 ± 3.5	58900 ± 3630	73600 ± 7430*
PGC1α	6.3 ± 1.7	4.8 ± 0.5	1260 ± 200	1360 ± 160	41 ± 7.5	79 ± 25	64 ± 11	90 ± 15
PGC1β	3310 ± 345	3610 ± 980	7.5 ± 1.1	9.8 ± 1.2	10 ± 1.3	8.6 ± 1.0	40 ± 10	40 ± 5
SREBP1	3190 ± 670	2910 ± 460	31 ± 6	46 ± 7	40 ± 1.6	33 ± 2.2*	7000 ± 2330	3270 ± 487
CHREBP	69 ± 15	54 ± 10	54 ± 8.1	80 ± 13	860 ± 142	1020 ± 270	2930 ± 1090	4880 ± 1260
SCD1	1530000 ± 321000	494000 ± 108000*	5210 ± 1860	6340 ± 500	1550 ± 803	606 ± 136	3710000 ± 779000	1410000 ± 248000*
ACC1	1011 ± 125	1017 ± 213	36 ± 7	30 ± 3.6	2.6 ± 0.68	1.7 ± 0.13		
ACC2	21700 ± 2300	16500 ± 4250	2.1 ± 1.0	1.2 ± 0.22	6.2 ± 0.64	5.7 ± 0.62	27900 ± 15000	14700 ± 3480
DGAT1	3310 ± 361	2220 ± 98*	1.0 ± 0.1	1.2 ± 0.14	227 ± 40	208 ± 40		
DGAT2	216000 ± 19200	. 167000 ± 19000	94 ± 8.5	115 ± 6.6	7.2 ± 1.3	9.6 ± 1.7	0.24 ± 0.07	0.15 ± 0.03
LXRα	49700 ± 3480	42100 ± 2040	32 ± 2.3	31 ± 3.9	273 ± 26	299 ± 65	1220 ± 396	1970 ± 387
CYP7A1	163000 ± 19100	190000 ± 35400	11086 ± 2380	12350 ± 3650				
FXR	25000 ± 1140	24800 ± 1410	24 ± 1.0	22 ± 3.2	45600 ± 14600	35300 ± 3080	2910 ± 374	2010 ± 175
ABCB11	103000 ± 7420	70300 ± 6570*	196 ± 17	217 ± 49	1.1 ± 0.3	2.4 ± 1.5	1.4 ± 0.3	2.6 ± 1.7
UCP1							324000 ± 28900	399000 ± 20400*
UCP2			0.22 ± 0.04	0.29 ± 0.05	0.52 ± 0.09	0.53 ± 0.13		
UCP3	38 ± 8.9	53 ± 17			143 ± 26	90 ± 6.4		

Data represent mean ± SEM of 5 mice per group.

Cell Metab. Author manuscript; available in PMC 2011 July 29.

* $P < 0.05$ compared with wild type (WT) control mice.